Ca^{2+} influx and the store-operated Ca^{2+} entry pathway undergo regulation during mouse oocyte maturation

Banyoon Cheon[a,b], Hoi-Chang Lee[b], Takuya Wakai[c], and Rafael A. Fissore[a,b]
[a]Molecular and Cellular Biology Program and [b]Department of Veterinary and Animal Sciences, University of Massachusetts, Amherst, MA 01002; [c]Department of Bioscience, Tokyo University of Agriculture, 1-1-1 Setagaya-ku, Tokyo 156-8502, Japan

ABSTRACT **In preparation for fertilization, mammalian oocytes undergo optimization of the mechanisms that regulate calcium homeostasis. Among these changes is the increase in the content of the Ca^{2+} stores ($[Ca^{2+}]_{ER}$), a process that requires Ca^{2+} influx. Nevertheless, the mechanism(s) that mediates this influx remains obscure, although is known that $[Ca^{2+}]_{ER}$ can regulate Ca^{2+} influx via store-operated Ca^{2+} entry (SOCE). We find that during maturation, as $[Ca^{2+}]_{ER}$ increases, Ca^{2+} influx decreases. We demonstrate that mouse oocytes/eggs express the two molecular components of SOCE—stromal interaction molecule 1 (Stim1) and Orai1—and expression of human (h) Stim1 increases Ca^{2+} influx in a manner that recapitulates endogenous SOCE. We observe that the cellular distribution of hStim1 and hOrai1 during maturation undergoes sweeping changes that curtail their colocalization during the later stages of maturation. Coexpression of hStim1 and hOrai1 enhances influx throughout maturation but increases basal Ca^{2+} levels only in GV oocytes. Further, expression of a constitutive active form of hStim1 plus Orai1, which increases basal Ca^{2+} throughout maturation, disturbs resumption of meiosis. Taken together, our results demonstrate that Ca^{2+} influx and SOCE are regulated during maturation and that alteration of Ca^{2+} homeostasis undermines maturation in mouse oocytes.**

Monitoring Editor
Marianne Bronner
California Institute of Technology

Received: Jan 30, 2013
Accepted: Feb 27, 2013

INTRODUCTION

Changes in the intracellular concentration of free calcium ($[Ca^{2+}]_i$) represent an important signaling mechanism involved in a wide range of cellular events, including muscle contraction, secretion, neurotransmission, and cell death (Berridge *et al.*, 2000). $[Ca^{2+}]_i$ signaling also plays a dominant role during fertilization in all species examined (Stricker, 1999; Runft *et al.*, 2002; Malcuit *et al.*, 2006; Swann *et al.*, 2006). In mammals, the sperm-induced $[Ca^{2+}]_i$ signal adopts a pattern of brief $[Ca^{2+}]_i$ rises interspersed among long intervals of basal concentration, which are referred to as $[Ca^{2+}]_i$ oscillations. The oscillations are believed to be initiated by a sperm-specific phospholipase C (PLC), PLC zeta1 (ζ), after fusion of the gametes (Saunders *et al.*, 2002). PLCζ is believed to hydrolyze phosphatidylinositol 4,5-bisphosphate (PIP_2), resulting in the production of 1,4,5-inositol-trisphosphate (IP_3), the ligand for IP_3R1, the Ca^{2+} channel located in the endoplasmic reticulum (ER), the egg's main Ca^{2+} store (Miyazaki *et al.*, 1992; Miyazaki, 2006; Ducibella and Fissore, 2008). Activation of this pathway causes the initial intracellular Ca^{2+} release, but persistence of the oscillations requires Ca^{2+} influx, as without external Ca^{2+} ($[Ca^{2+}]_e$) only a few rises occur after sperm entry (Kline and Kline, 1992). Notwithstanding the importance of Ca^{2+} influx, the mechanisms that underlie it during mammalian fertilization are unknown.

Fertilization in most vertebrate species happens at the metaphase II stage of meiosis (MII), although changes in Ca^{2+} homeostasis that

This article was published online ahead of print in MBoC in Press (http://www.molbiolcell.org/cgi/doi/10.1091/mbc.E13-01-0065) on March 6, 2013.

Address correspondence to: Rafael A. Fissore (rfissore@vasci.umass.edu).

Abbreviations used: AP, antigenic peptide; BSA, bovine serum albumin; CAD, CRAC-activating domain; $[Ca^{2+}]_e$, external Ca^{2+}; $[Ca^{2+}]_{ER}$, Ca^{2+} in endoplasmic reticulum; $[Ca^{2+}]_i$, intracellular concentration of free calcium; CIP, calf intestine phosphatase; CRAC, Ca^{2+} release-activated Ca^{2+}; cRNA, complementary RNA; CZB, Chatot, Ziomek, and Bavister medium; EGTA, ethylene glycol tetraacetic acid; ER, endoplasmic reticulum; Fura-2AM, Fura-2 acetoxymethyl ester; GV, germinal vesicle; GVBD, germinal vesicle breakdown; HCZB, HEPES-buffered CZB; IBMX, 3-isobutyl-1-methylxanthine; IP_3, 1,4,5-inositol-trisphosphate; IP_3R1, 1,4,5-inositol-trisphosphate receptor 1; MI, metaphase I; MII, metaphase II; mRFP, modified red fluorescent protein; PIP_2, phosphatidylinositol 4,5-bisphosphate; PM, plasma membrane; PMSG, pregnant mare serum gonadotropin; PVA, polyvinyl alcohol; SEM, standard error of mean; SERCA, sarcoendoplasmic reticulum Ca^{2+}-ATPase; SOCE, store-operated Ca^{2+} entry; Stim1, stromal interaction molecule1; TG, thapsigargin; TL-HEPES, Tyrode's lactate solution; WGA, wheat germ agglutinin; YFP, yellow fluorescent protein.

© 2013 Cheon *et al.* This article is distributed by The American Society for Cell Biology under license from the author(s). Two months after publication it is available to the public under an Attribution–Noncommercial–Share Alike 3.0 Unported Creative Commons License (http://creativecommons.org/licenses/by-nc-sa/3.0).

"ASCB®," "The American Society for Cell Biology®," and "Molecular Biology of the Cell®" are registered trademarks of The American Society of Cell Biology.

occur before this stage during maturation enable eggs to mount $[Ca^{2+}]_i$ oscillations. Fully grown mammalian oocytes are arrested at the germinal vesicle stage (GV) and are endowed with Ca^{2+} stores ($[Ca^{2+}]_{ER}$) low in Ca^{2+} reserves. As maturation ensues after the luteinizing hormone surge, $[Ca^{2+}]_{ER}$ increases steadily until the MII stage (Tombes *et al.*, 1992; Jones *et al.*, 1995), enhancing IP_3R1-mediated Ca^{2+} release and promoting the acquisition of fertilization-like oscillations (Miyazaki *et al.*, 1993; Mehlmann and Kline, 1994). The mechanism(s) that underlie this increase in $[Ca^{2+}]_{ER}$ and the plasma membrane (PM) channels that underpin the Ca^{2+} influx are unknown, although insights may be gleaned from the spontaneous $[Ca^{2+}]_i$ oscillations displayed by GV oocytes (Carroll and Swann, 1992; Carroll *et al.*, 1994). These oscillations require Ca^{2+} influx and end approximately as the resumption of meiosis begins (Carroll and Swann, 1992), which is when the first increase in $[Ca^{2+}]_{ER}$ content is noted (Jones *et al.*, 1995). These results both predict an association between $[Ca^{2+}]_{ER}$ content and Ca^{2+} influx, which is reminiscent of the mechanism believed to underlie store-operated Ca^{2+} entry (SOCE; Putney, 1986; Hoth and Penner, 1993) and active regulation of Ca^{2+} influx during maturation.

SOCE was first proposed as a means for cells to refill Ca^{2+} stores after Ca^{2+} release induced by agonist stimulation (Putney, 1986). Subsequent studies showed that depletion of $[Ca^{2+}]_{ER}$ caused by inhibitors of the sarcoplasmic/endoplasmic reticulum Ca^{2+}-ATPase (SERCA) pumps such as thapsigargin (TG) also triggered Ca^{2+} influx, demonstrating the prevalence of SOCE in somatic cells (Takemura *et al.*, 1989; Hoth and Penner, 1993; Zweifach and Lewis, 1993; Hsu *et al.*, 2001). Subsequent electrophysiological studies revealed unique properties of this current, which was named I_{CRAC} (Hoth and Penner, 1993; Zweifach and Lewis, 1993; Parekh *et al.*, 1997; Putney, 2009). Although unknown for many years, the molecular effectors of SOCE have been identified, and two components, stromal interaction molecule 1 (Stim1), which acts as the ER Ca^{2+} sensor (Liou *et al.*, 2005; Roos *et al.*, 2005; Collins and Meyer, 2011), and Orai1, the PM channel that mediates Ca^{2+} influx upon Stim1-induced oligomerization (Feske *et al.*, 2006; Vig *et al.*, 2006), are believed to coordinate Ca^{2+} influx after Ca^{2+} release. The presence of SOCE has been well characterized during the early stages of maturation in *Xenopus* oocytes (Yu *et al.*, 2009), and Ca^{2+} influx has been described in mammalian eggs during fertilization and after addition of TG (Kline and Kline, 1992; McGuinness *et al.*, 1996; Mohri *et al.*, 2001), although the mechanism(s) and molecules underlying this Ca^{2+} entry remain to be identified. Consistent with this, detection of transcripts for Stim1 and Orai1 has been reported in mammalian oocytes, although protein expression and cellular distribution during maturation require additional characterization (Gomez-Fernandez *et al.*, 2009, 2012; Koh *et al.*, 2009; Wang *et al.*, 2012).

Although Ca^{2+} influx is required for $[Ca^{2+}]_i$ oscillations at the GV stage, its contributions to the filling of $[Ca^{2+}]_{ER}$ have not been carefully examined. Further, the role of $[Ca^{2+}]_i$ changes during oocyte maturation is unclear. For instance, in mouse GV oocytes suppression of spontaneous oscillations with the Ca^{2+} chelator BAPTA-AM did not affect resumption of meiosis, although it caused cell cycle arrest at metaphase I (MI) of meiosis (Tombes *et al.*, 1992). In porcine and bovine oocytes, addition of BAPTA-AM prevented resumption of meiosis, and removal of $[Ca^{2+}]_e$ precluded progression of meiosis beyond the MI stage (Homa, 1991; Kaufman and Homa, 1993). Remarkably, in *Xenopus* oocytes, in which SOCE is inactivated during maturation (Machaca and Haun, 2000), increased Ca^{2+} influx by elevation of $[Ca^{2+}]_e$ and persistent increase in $[Ca^{2+}]_i$ delayed resumption of meiosis and caused spindle abnormalities (Sun and Machaca, 2004). Whether enhanced Ca^{2+} influx and persistent elevation of basal $[Ca^{2+}]_i$ affect the initiation or progression of maturation in mammalian oocytes has not been examined.

In this study in mouse oocytes we investigate whether Ca^{2+} influx contributes to the filling of $[Ca^{2+}]_{ER}$ during maturation and whether it is differentially regulated during this process. We also study whether SOCE contributes to this influx, as well as the expression of the molecular components of SOCE and their regulation during maturation. Finally, we evaluate the impact of persistently elevated $[Ca^{2+}]_i$ on resumption and progression of meiosis.

RESULTS

Spontaneous Ca^{2+} influx is suppressed during maturation in parallel with the increase of ER Ca^{2+} store

To gain insight into the mechanism and molecular effectors that mediate Ca^{2+} influx in mouse oocytes and eggs, we ascertained whether Ca^{2+} influx across the PM was required for the increase in $[Ca^{2+}]_{ER}$ that occurs during the transition from the GV to the germinal vesicle breakdown (GVBD) stage (Jones *et al.*, 1995). To accomplish this, GV oocytes were allowed to transition to the GVBD stage in the presence/absence of extracellular Ca^{2+} (1.7 mM). We estimated $[Ca^{2+}]_{ER}$ levels after addition of TG 4 h after the removal of 3-isobutyl-1-methylxanthine (IBMX). In the presence of extracellular Ca^{2+}, $[Ca^{2+}]_{ER}$ increased significantly in GVBD oocytes (Figure 1A, top, left and right), although this was not the case when maturation was initiated in nominal Ca^{2+}-free medium (Figure 1A, bottom, right). These results therefore demonstrate that $[Ca^{2+}]_e$ is required for $[Ca^{2+}]_{ER}$ increase during maturation.

We next examined whether the Ca^{2+} entry pathway(s) that mediate Ca^{2+} influx in GV oocytes are also functional in MII eggs, as both of these cellular stages are known to support oscillations. We incubated GV oocytes and MII eggs in nominal Ca^{2+}-free media and soon thereafter sequentially added 2 and 5 mM $CaCl_2$ while we monitored $[Ca^{2+}]_i$ responses. Although most GV oocytes responded to the addition of $CaCl_2$ by displaying a noticeable $[Ca^{2+}]_i$ rise and in some cases oscillations (Figure 1B, left), MII eggs displayed no such changes (Figure 1B, middle). We next examined whether the Ca^{2+} entry at the GV stage could be abrogated by pretreatment with 50 µM 2-APB, a pharmacological agent that has been shown to regulate SOCE (DeHaven *et al.*, 2008); addition of 2-APB prevented the increase in $[Ca^{2+}]_i$ after the addition of either concentration of $CaCl_2$ (Figure 1B, right).

The inhibitory effect of 2-APB and the low $[Ca^{2+}]_{ER}$ levels in GV oocytes suggested that SOCE may be involved, at least in part, in mediating Ca^{2+} entry in GV oocytes. Accordingly, we investigated whether Ca^{2+} influx at the GV stage could be modified by exposure to TG before $CaCl_2$ add back, a method commonly used to test SOCE in somatic cells (Bird *et al.*, 2008; DeHaven *et al.*, 2008). Although 3 of 20 untreated oocytes showed large and prolonged $[Ca^{2+}]_i$ responses after addition of $CaCl_2$, the majority of oocytes, 9 and 8 of 20, respectively, showed moderate or minor responses (Figure 1C, left). Conversely, TG-exposed oocytes uniformly responded to the addition of $CaCl_2$ with robust $[Ca^{2+}]_i$ responses (Figure 1C, right). Taken together, these results show that Ca^{2+} entry is functionally regulated during mouse oocyte maturation and that SOCE is one of the underlying mechanisms of Ca^{2+} influx at the GV stage.

$[Ca^{2+}]_{ER}$ content and Ca^{2+} influx undergo distinct regulation during mouse oocyte maturation

The previous findings led us to investigate the function of SOCE throughout oocyte maturation, using the TG and $CaCl_2$ add-back method. Addition of TG, as expected, caused an increase in $[Ca^{2+}]_i$ that became gradually higher as maturation progressed (Figure 2, A and C; $p < 0.05$), which is in agreement with previous

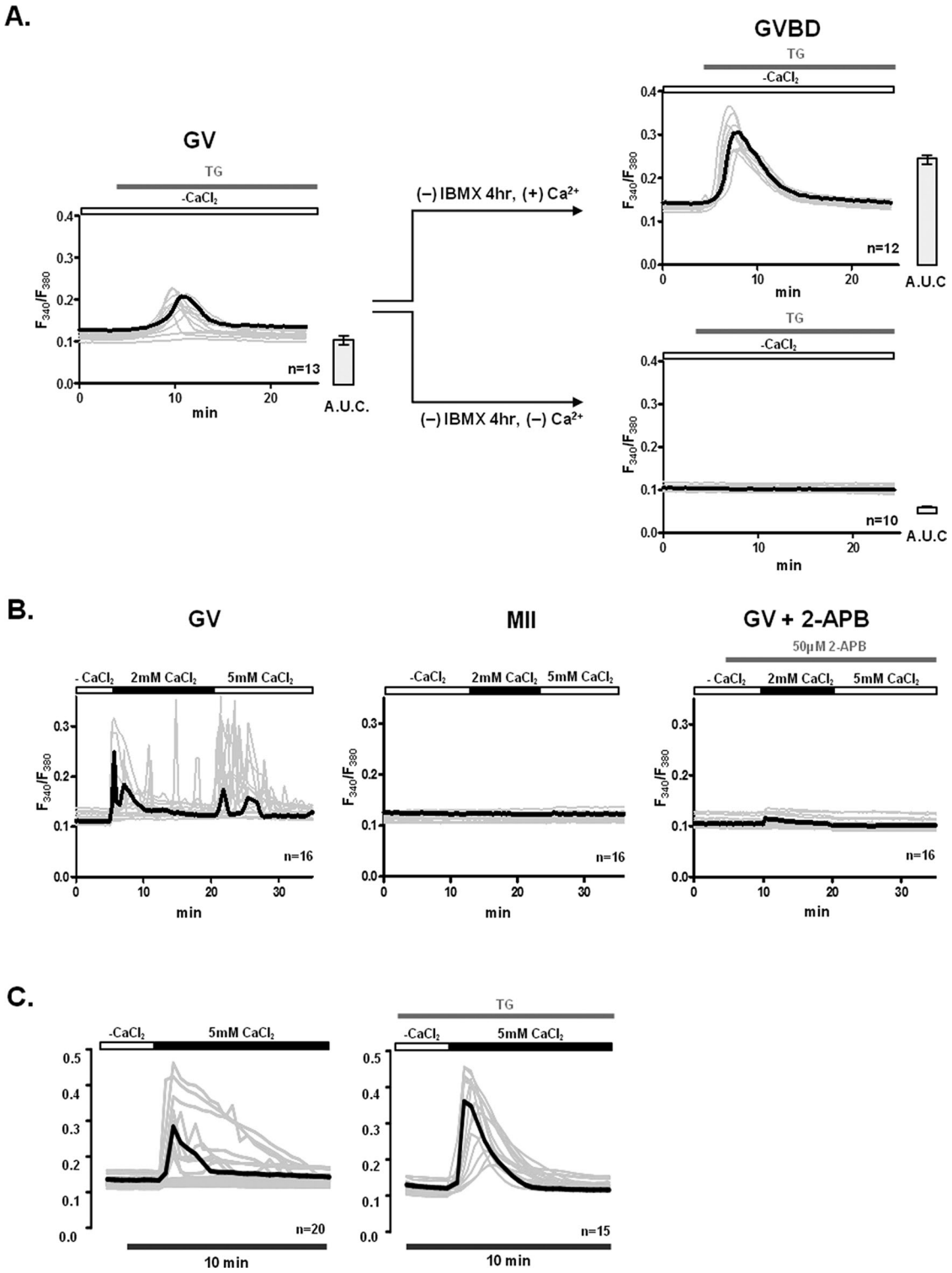

FIGURE 1: $[Ca^{2+}]_e$ and Ca^{2+} influx are required to fill $[Ca^{2+}]_{ER}$ in oocytes. The underlying Ca^{2+} influx mechanism(s) are inactivated during maturation and are sensitive to 2-APB and TG at the GV stage. (A) The contribution of extracellular Ca^{2+} to $[Ca^{2+}]_{ER}$ content was estimated in GVBD-stage oocytes after culturing GV oocytes for 4 h in media supplemented with 1.7 mM $CaCl_2$ or without supplementation, nominal Ca^{2+}-free medium. Release of $[Ca^{2+}]_{ER}$ was induced by addition of 10 μM TG. All $[Ca^{2+}]_i$ responses are shown in the graphs, and the bold trace in each graph represents the mean response; bar graphs to the right of each Ca^{2+} panel denote mean ± SEM of $[Ca^{2+}]_{ER}$ content estimated as area under the curve. (B) Spontaneous Ca^{2+} influx was measured in GV oocytes and MII eggs. Oocytes and eggs were placed in Ca^{2+}-free conditions, after which 2 and 5 mM $CaCl_2$ were successively added. Given that only GV oocytes showed Ca^{2+} influx, they were pretreated with 50 μM 2-APB for 5 min before addition of $CaCl_2$ to prevent influx. (C) Ca^{2+} influx was promoted by addition of $CaCl_2$ into GV oocytes with and without prior treatment with TG. GV oocytes were placed in nominal Ca^{2+}-free media or exposed to 10 μM TG for 30 min in nominal Ca^{2+}-free medium to deplete $[Ca^{2+}]_{ER}$, after which 5 mM $CaCl_2$ was added. Representative traces are shown, and bold trace represents mean response.

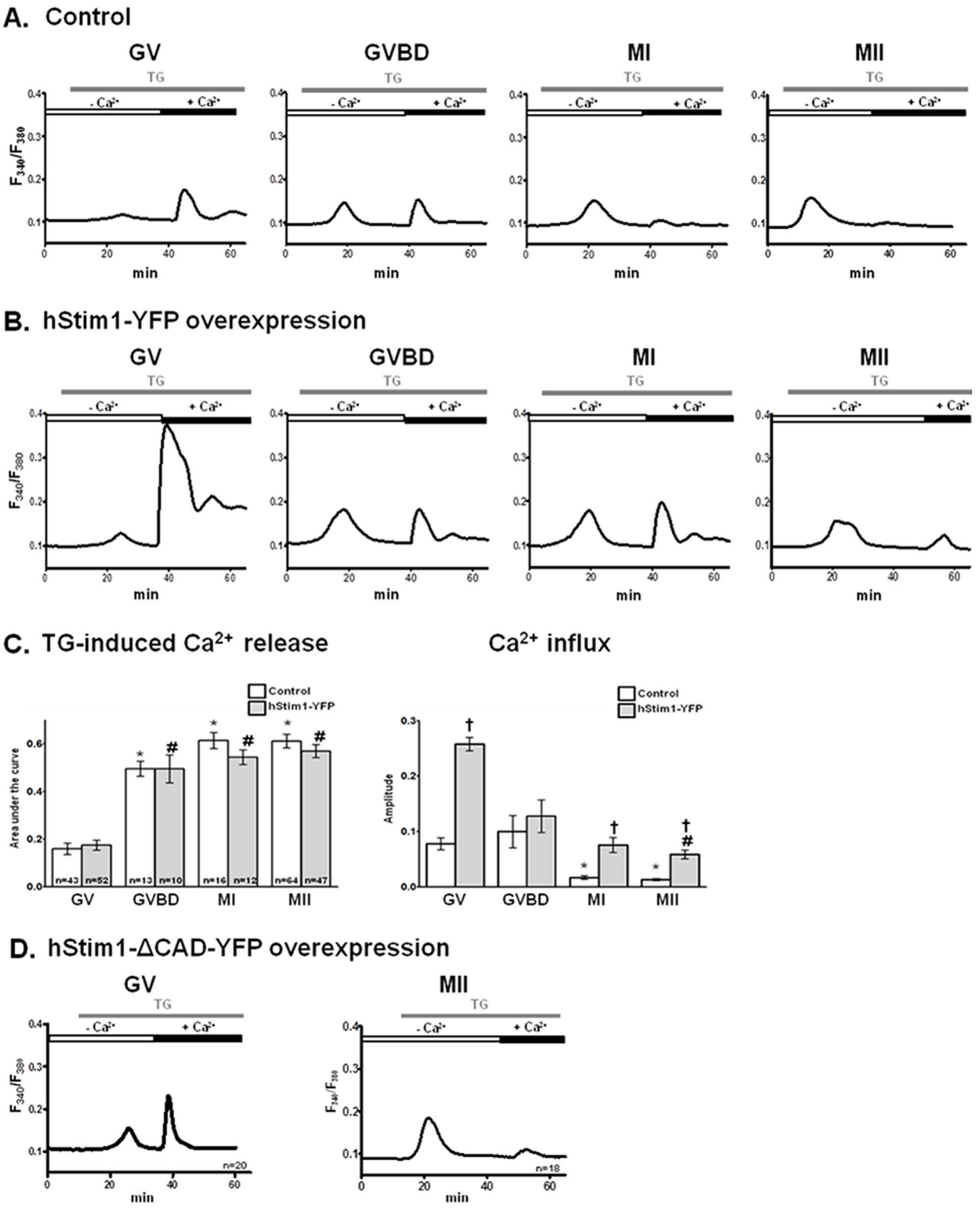

FIGURE 2: $[Ca^{2+}]_{ER}$ content increases, whereas Ca^{2+} influx induced by TG, SOCE, decreases during oocyte maturation. $[Ca^{2+}]_{ER}$ content was estimated from the $[Ca^{2+}]_i$ responses caused by addition of 10 μM TG in oocytes incubated in Ca^{2+}-free medium, and Ca^{2+} influx was estimated by the $[Ca^{2+}]_i$ rise generated by the addition of 5 mM $CaCl_2$ soon after the TG-induced $[Ca^{2+}]_i$ rise had subsided. Representative $[Ca^{2+}]_i$ traces are shown for control oocytes (A) or for oocytes expressing hStim1-YFP (B). (C) TG- and $CaCl_2$-induced $[Ca^{2+}]_i$ changes were quantified, and data are presented in bar graphs as mean ± SEM. Control and hStim1-YFP–expressing oocytes are displayed in open and gray columns, respectively, and the number of oocytes evaluated is shown within each bar. *,#Stages significantly different from the GV-stage values within treatment group. †Significant differences within the same meiotic stage but between treatments ($p < 0.05$). (D) TG-induced $[Ca^{2+}]_i$ responses and subsequent Ca^{2+} influx in oocytes and eggs expressing hStim1-ΔCAD-YFP, an Stim1 variant incapable of interacting with Orai1.

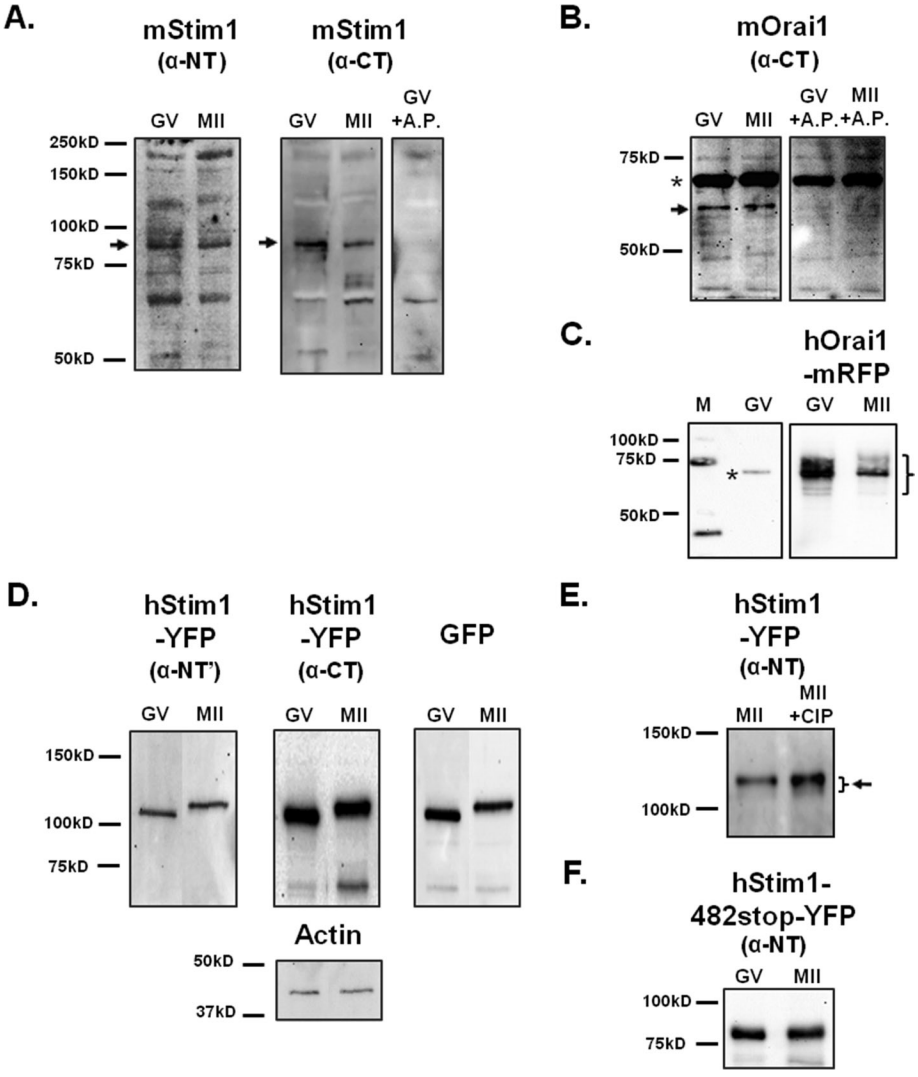

FIGURE 3: Mouse oocytes express Stim1 and Orai1. (A, B) The expression of Stim1 and Orai1 molecules was probed using lysates of GV oocytes (n = 100 and 200, respectively) and MII (n = 100 and 200, respectively) eggs and specific antibodies. (A) Left and middle, black arrows point to the band corresponding to Stim1. An antigenic peptide was used to confirm the specificity of the anti–C-terminus Stim1 antibody. (B) Right, black arrow points to the band that represents Orai1. The upper band of ~68 kDa marked with an asterisk is believed to be nonspecific reactivity, as it was not abolished by pretreatment with the antigenic peptide. (C) hOrai1-mRFP expression (n = 16 GV oocytes/MII eggs) was analyzed in overexpressing cells using the same antibody. (D) Heterologous expression of hStim1-YFP was demonstrated in lysates of oocytes/eggs (n = 45) using the anti–N-terminus and anti–C-terminus Stim1 antibodies and an anti-GFP antibody. The actin protein was probed as a loading control (bottom, middle). (E) To examine the possible phosphorylation of hStim1-YFP in mouse oocytes, lysates of hStim1-YFP–expressing MII oocytes (n = 18) were incubated with or without calf intestine phosphatase and then immunoblotted with anti-Stim1 antibody (right). The presence of hStim1 is denoted by an arrow, and the bracket denotes the presence of polypeptides of different MWs. (F) hStim1–482-stop-YFP–overexpressing GV and MII cells (n = 18) were probed with the anti–N-terminus Stim1 antibody, and blots are shown.

reports (Kline and Kline, 1992; Jones *et al.*, 1995) and suggests increasing $[Ca^{2+}]_{ER}$ content with progression of maturation. In contrast, after $CaCl_2$ addition, Ca^{2+} influx progressively decreased during maturation, with GV- and GVBD-stage oocytes displaying greater Ca^{2+} influx than MI and MII eggs (Figure 2, A and C; $p < 0.05$), demonstrating gradual inactivation of Ca^{2+} entry with progression of maturation.

The inverse relationship between $[Ca^{2+}]_{ER}$ content and Ca^{2+} entry during maturation indicates the participation of SOCE as one of the mechanisms involved in Ca^{2+} homeostasis in mouse oocytes. Remarkably, our results suggest that SOCE is progressively disabled during maturation. To extend these observations, we injected GV-stage oocytes with *hStim1*–yellow fluorescent protein (YFP) cRNA, the Ca^{2+} sensor component of SOCE, and examined the effects of such injections on $[Ca^{2+}]_{ER}$ and Ca^{2+} influx during different stages of maturation. hStim1 and mStim1 are highly homologous, sharing ~97% of the amino acids at the whole-protein level and 99% of the amino acids in the CRAC-activating domain (CAD), which is the domain that directly interacts with Orai1 (Park *et al.*, 2009). Therefore hStim1-YFP overexpression was expected to mimic mStim1 function. Expression of hStim1-YFP did not affect $[Ca^{2+}]_{ER}$ content throughout maturation (Figure 2, B and C, left), at least as estimated by our approach, but clearly enhanced Ca^{2+} influx in all stages of maturation, especially in GV oocytes (Figure 2, B and C, right; $p < 0.05$). To demonstrate that the enhanced influx was due to interaction of hStim1 with endogenous Orai1, we injected oocytes with hStim1-ΔCAD-YFP mRNA, which cannot activate Orai1 (Park *et al.*, 2009); overexpression of hStim1-ΔCAD-YFP failed to enhance Ca^{2+} influx at any stage of maturation (Figure 2D). Collectively the data suggest that hStim1-YFP overexpression broadly recapitulates the regulation of $[Ca^{2+}]_{ER}$ and Ca^{2+} influx observed in mouse oocytes, suggesting that SOCE is operational during mouse oocyte maturation, although it is seemingly inactivated at the most advanced stages of meiosis.

Stim1 and Orai1 are expressed in mouse oocytes

We next examined in mouse oocytes/eggs the expression of the two molecular effectors of SOCE—Stim1 and Orai1. Two different anti-Stim1 antibodies were used for Western blotting, and both antibodies detected a band of ~90 kDa in GV and MII stages (Figure 3A, left and center), which is the reported molecular weight (MW) of Stim1 (Darbellay *et al.*, 2011); the observed reactivity was likely Stim1's, as preincubation of the anti–C-terminus antibody with an antigenic peptide specifically obliterated recognition of this band (Figure 3A, right). Expression of Orai1 was also detected in mouse eggs (Figure 3B, left) with an approximate MW of 56 kDa, which, although higher than predicted for the native protein, is consistent with the MW of the protein in some mammalian tissues (Balghi *et al.*, 2011); Orai1 has been shown to be glycosylated in somatic cells (Prakriya *et al.*, 2006; Gwack *et al.*, 2007). Preincubation of the antibody with

its antigenic peptide abrogated the reactivity of the 56 kDa band but not that of a prominent higher, nonspecific band (Figure 3B, right; asterisk), confirming the specificity of the antibody. Further, the same antibody detected expression of hOrai1–monomeric red fluorescent protein (mRFP) in oocytes and eggs, where it detected several polypeptides ranging in MW from ~52 to 82 kDa, likely the reflection of various degrees of glycosylation (Figure 3C).

To confirm the functional results obtained by injection of hStim1-YFP cRNA, we examined the expression of hStim1-YFP in GV and MII oocytes. Both anti-Stim1 antibodies recognized a band at ~105 kDa, which is consistent with the MW of hStim1 and the added MW of YFP (Figure 3D, left and middle); an anti-YFP antibody recognized the same bands (Figure 3D, right). Actin was used as loading control, and Western blotting against it revealed approximate equal loading of the samples (Figure 3D, bottom, middle). In all cases, hStim1-YFP migration was more retarded in MII eggs than in GV oocytes (Figure 3D), suggesting phosphorylation of hStim1-YFP, as reportedly occurs in *Xenopus* oocytes and in mammalian somatic cells (Smyth *et al.*, 2009; Yu *et al.*, 2009). To ascertain whether this was also the case in our system, we injected hStim1-YPF cRNAs into GV oocytes; these cells matured to the MII stage, at which time lysates were prepared and either left untreated or treated with alkaline phosphatase (AP) to induce widespread dephosphorylation. Compared to untreated controls, the AP-treated hStim1-YPF displayed a smeared migration, which suggests different degrees of phosphorylation, and higher reactivity (Figure 3E), which is possibly due to better antibody recognition, as the antibody's epitope falls within this domain. To confirm this observation, we injected hStim1-482stop-YFP cRNA, which encodes for a protein that lacks all the C-term M-phase kinase phosphorylation sites (Smyth *et al.*, 2009); hStim1-482stop did not undergo a mobility shift during maturation (Figure 3F). Collectively our data show that the components of SOCE are expressed in mouse oocytes/eggs and that during maturation hStim1 undergoes phosphorylation.

hStim1-YFP and hOrai1-mRFP undergo changes in distribution during oocyte maturation

Such findings led us to examine whether the decline in Ca^{2+} influx during maturation coincided with changes in the cellular distribution of Stim1 and Orai1. To follow their distribution, we injected oocytes with hStim1-YFP or hOrai1-mRFP mRNAs. All oocytes were injected at the GV stage and remained at this stage in media supplemented with IBMX for variable times, so that by 20 h postinjection all stages of maturation could be simultaneously examined. hStim1-YFP underwent marked changes in distribution with progression of meiosis. For example, at the GV stage, hStim1-YFP displayed a "patched" distribution, with these patches spread throughout the cell (Figure 4A). In GVBD oocytes, ~4 h after removal of IBMX, large internal patches were still observed in most oocytes (Figure 4B, top), but in ~30% of the cells the distribution of hStim1 became more diffuse, although some patches remained around the spindle area (Figure 4B, bottom). As maturation progressed, the distribution of hStim1 became more disperse and acquired a pattern consistent with its ER localization (Figure 4, C and D, top), although a small number of MI and MII oocytes still showed internal patches of smaller size (Figure 4, C and D, bottom); ER distribution was confirmed by injection of ds-Red ER cRNA (data not shown).

The distribution of hOrai1-mRFP also changed during maturation (Figure 4, E and F). For example, at the GV stage, hOrai1-mRFP was highly enriched at the PM, where it formed a near-perfect ring around the cell (Figure 4E), whereas at the MII stage, even though hOrai1-mRFP was still present there, its presence was weaker (Figure 4F); this apparent reduction of hOrai1-mRFP at the PM was accompanied by increased fluorescence in the subcortical area (Figure 4F; line and bar graphs below figures), suggesting recycling of the protein, as reported in *Xenopus* oocytes (Yu *et al.*, 2009, 2010). Collectively these results suggest that the molecular components of SOCE undergo cellular redistribution during maturation.

hStim1 puncta formation and colocalization with hOrai1 decrease during oocyte maturation

After depletion of $[Ca^{2+}]_{ER}$, Stim1 undergoes oligomerization and migration to the cell cortex, nearly reaching the PM, where these aggregates, also known as "puncta," recruit and gate Orai1 (Penna *et al.*, 2008; Park *et al.*, 2009). To assess whether the ability of Stim1 to undergo puncta formation and migration to the cortex changed during oocyte maturation, we treated hStim1-YFP–expressing GV and MII oocytes with TG and observed hStim1-YFP reorganization by confocal microscopy. To estimate the proximity of hStim1-YFP puncta to the PM, we used a diffusible dye, wheat germ agglutinin–Alexa 633, to stain the PM. After treatment with TG, hStim1 in GV oocytes readily formed distinct puncta that aligned along the PM (Figure 5, C and E), whereas this ability was severely reduced at the MII stage, along with the size of the puncta (Figure 5, D and F); the line graph to the right of Figure 5, E and F, shows the reduced intensity of the puncta in MII eggs. It is worth noting that even after TG, hStim1-YFP in MII eggs displayed a reticular organization, which was not observed in GV oocytes.

Research in somatic cells shows that Stim1 and Orai1 directly interact at the PM (Penna *et al.*, 2008; Park *et al.*, 2009). Using simultaneous expression of hStim1-YFP and hOrai1-mRFP mRNAs and confocal microscopy, we examined whether the distribution of these molecules overlapped and, if so, whether this property changed during maturation. Under resting conditions, hStim1 and hOrai1 showed their expected distributions in GV oocytes and MII eggs (Figure 5, G–I and M–O, respectively), and in GV oocytes some overlap between the molecules was noticeable (Figure 5, H and I). After addition of TG, hStim1 and hOrai1 showed extensive colocalization at the GV stage (Figure 5, K and L), although this was not evident in MII eggs (Figure 5, Q and R). Collectively the data show that the organization of hStim1 and hOrai1 follows distinct but parallel redistribution during oocyte maturation, which temporally coincides with the decline in Ca^{2+} influx during this process.

Coexpression of SOCE components enhances TG-induced Ca^{2+} influx at all stages of oocyte maturation

The diminished colocalization of hStim1 and hOrai1 in MII eggs after depletion of Ca^{2+} stores led us to examine whether Ca^{2+} influx was reduced at this stage. We expressed either component of SOCE alone or in combination and compared $[Ca^{2+}]_i$ responses in GV and MII stages using the TG and $CaCl_2$ add-back method. As shown in Figure 6A, expression of hStim1 alone enhanced influx in both stages of maturation but to a greater extent in GV than in MII, which is consistent with our previous results. Expression of hOrai1, on the other hand, failed to modify influx at either stage, whereas hStim1 and hOrai1 coexpression increased Ca^{2+} influx in both stages, although the $[Ca^{2+}]_i$ rise was considerably smaller in MII eggs, consistent with the reduced colocalization of hStim1 and hOrai1 at this stage.

Expression of SOCE components alters basal Ca^{2+} homeostasis during oocyte maturation

We next examined whether expression/coexpression of the SOCE components changed basal $[Ca^{2+}]_i$ levels under natural regular

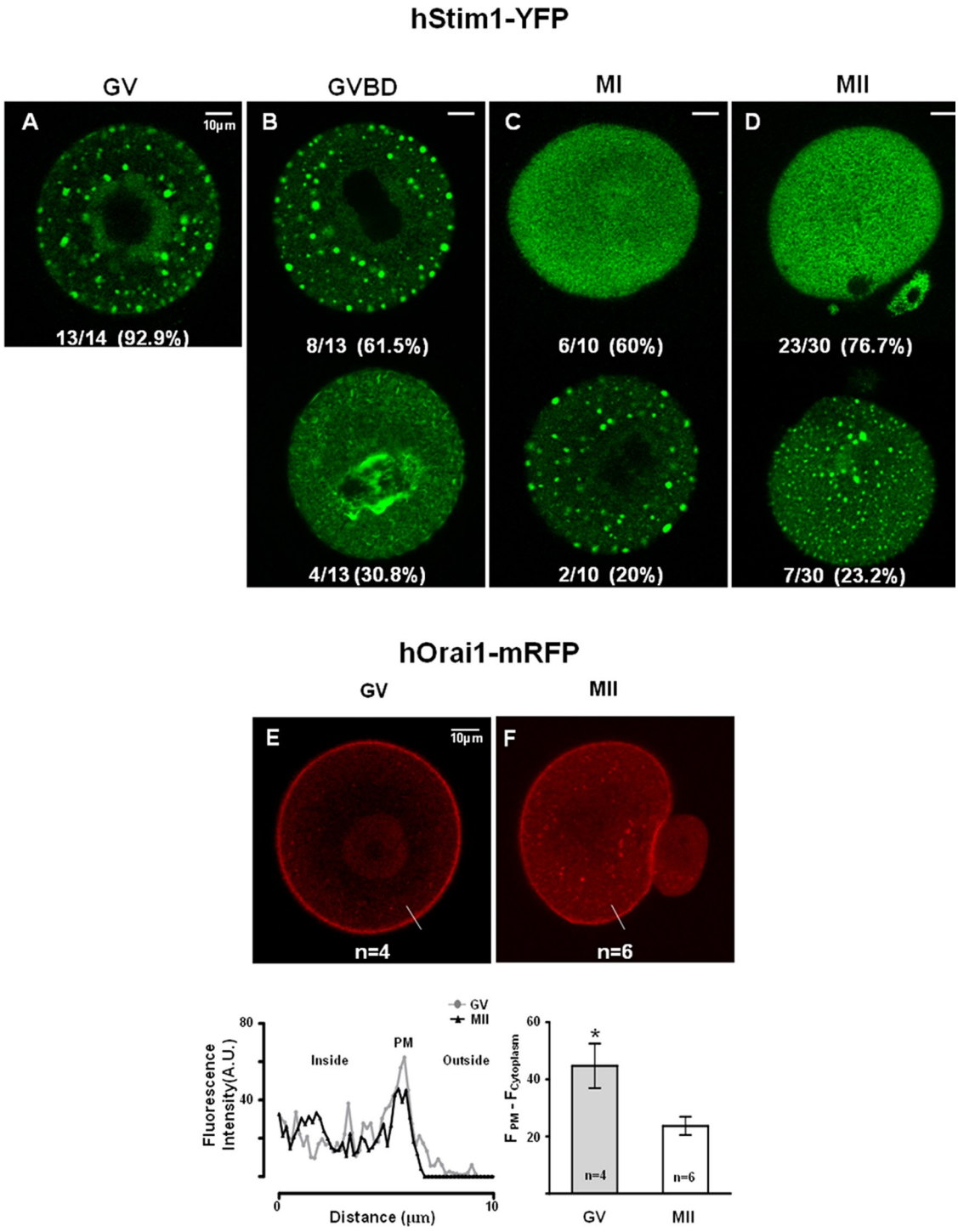

FIGURE 4: The distribution and organization of hStim1-YFP and hOrai1-mRFP change during oocyte maturation. (A–D) The distribution of hStim1-YFP was examined using confocal microscopy from images taken at the equatorial plane of live hStim1-YFP–expressing oocytes. The number of oocytes examined at each stage is shown at the bottom of each representative image. hStim1-YFP displayed two distinct patterns of organization in all stages of maturation except the GV stage; the most representative configurations are shown, along with the proportion of oocytes/eggs exhibiting the particular pattern. (E, F) The distribution of hOrai1 was examined as in the foregoing in GV and MII oocytes expressing hOrai1-mRFP. Intensity profiles of the line scans drawn in oocytes and eggs are shown below E, and a bar graph displaying the relative intensity of Orai1 signal between PM and cytoplasm is shown below F. Scale bar, 10 μm.

conditions, that is, without emptying the stores and under normal external Ca^{2+} concentration, ~1.7 mM $CaCl_2$. In control GV oocytes, basal $[Ca^{2+}]_i$ remained steady, as the fluorescence ratio of ~0.1 remained unchanged until the MII stage (Figure 6B, top, left). Expression of hStim1 increased baseline $[Ca^{2+}]_i$ in GV oocytes ($p < 0.05$), although by the MII stage basal $[Ca^{2+}]_i$ had returned to levels that were indistinguishable from those of noninjected controls (Figure 6B, top, right). Coexpression of hStim1 and hOrai1

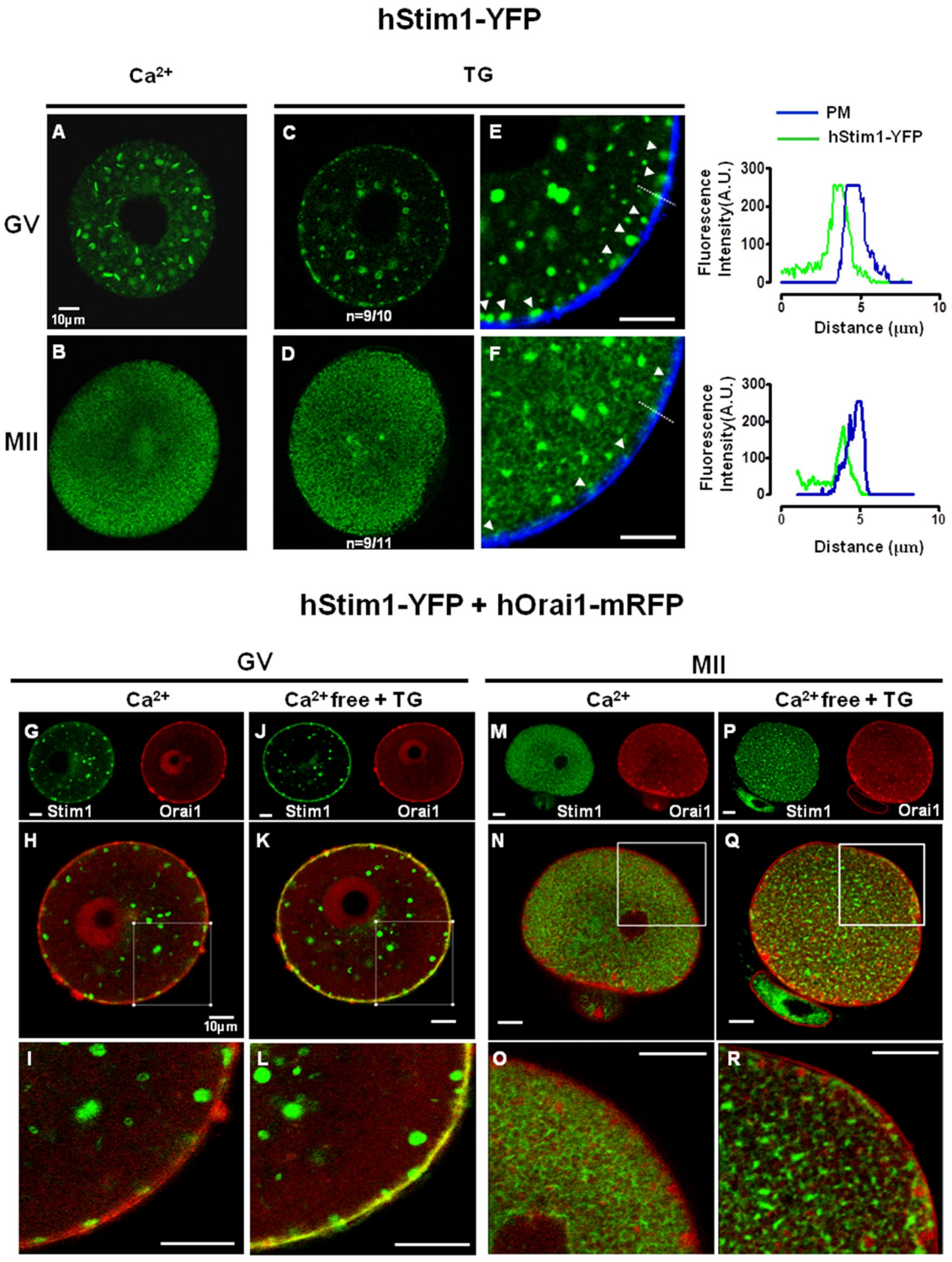

FIGURE 5: hStim1 puncta formation and colocalization with hOrai1 decreases during oocyte maturation. (A, B) Under control conditions, hStim1-YFP forms internal aggregates in GV oocytes, whereas in MII eggs it acquires a more homogenous, ER-like organization. After depletion of $[Ca^{2+}]_{ER}$, hStim1-YFP undergoes "puncta" formation in GV oocytes (C), whereas hStim1-YFP distribution is hardly changed in MII oocytes (D). Arrowheads point to hStim1-YPF puncta (E, F), and line graphs depicting the fluorescence intensity of these puncta, marked with a broken line, are shown to the right of E and F. (E, F) The proximity of the hStim1-YFP puncta/aggregates to the PM was estimated by staining the PM with wheat germ agglutinin–Alexa 664. hStim1-YPF puncta are bigger and more numerous in GV oocytes than in MII eggs. (G–R) Confocal images before and after TG treatment of GV oocytes (G–L) and MII eggs (M–R) expressing hStim1-YFP+hOrai1-mRFP. The same oocytes/eggs were imaged before and after TG. Top, separate fluorescent channels; middle, merged images; bottom, amplified regions of these are. hStim1 and hOrai1 display extensive overlap after the addition of TG in GV oocytes (K, L), but the overlap is negligible at the MII stage (Q, R). Scale bar, 10 μm.

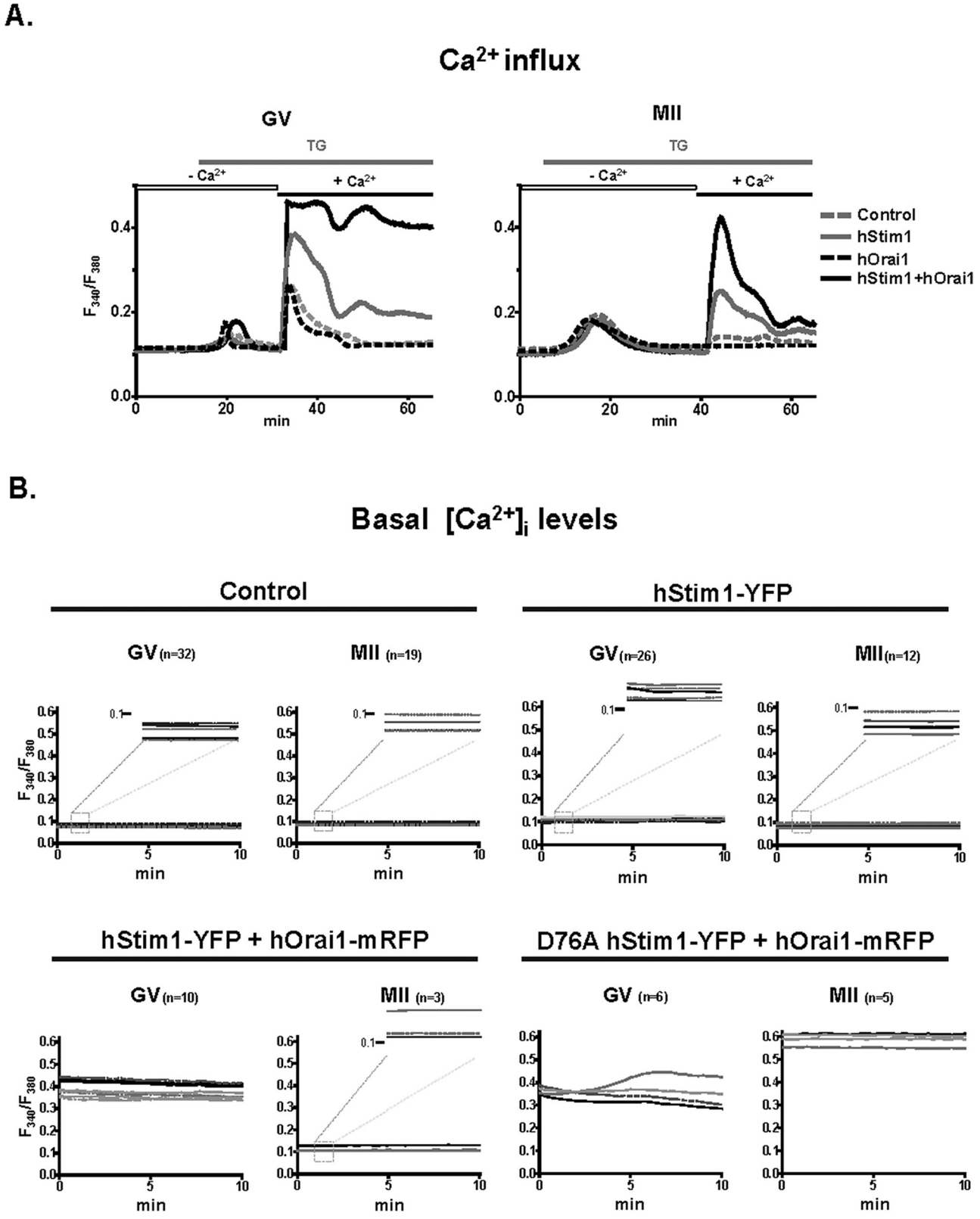

FIGURE 6: Overexpression of SOCE components alters Ca^{2+} homeostasis. (A) Expression of hStim1-YFP+hOrai1-mRFP increased Ca^{2+} influx in both GV and MII cells after TG and $CaCl_2$ add-back, although the increase was greater and more prolonged in GV oocytes. Expression of hStim1-YFP also increased Ca^{2+} influx in both GV and MII stages but to a lesser extent, whereas hOrai1 had no effect. (B) Expression of hStim1 or hStim1+hOrai1 differentially increased basal $[Ca^{2+}]_i$ during maturation. Baseline $[Ca^{2+}]_i$ traces in control (top, left), hStim1-YFP–expressing (top, right), hStim1-YFP+hOrai1-mRFP–expressing (bottom, left), and D76A hStim1-YFP+ hOrai1-mRFP–expressing (bottom, right) oocytes. Insets in each treatment depict a magnified version of the *y*-axis at the 0.1 mark so that minor differences in basal $[Ca^{2+}]_i$ between GV and MII stages can be appreciated for some of the treatments.

dramatically increased basal $[Ca^{2+}]_i$ at the GV stage ($p < 0.05$), and although basal $[Ca^{2+}]_i$ levels were reduced by the MII stage, they remained higher than for controls (Figure 6B, bottom, left). Taken together, these results demonstrate that spontaneous Ca^{2+} influx is differentially regulated during mouse oocyte maturation and is greatest at the GV stage, consistent with the presence of spontaneous oscillations at this stage (Carroll and Swann, 1992).

To ascertain whether the downturn of Ca^{2+} influx was likely due to increasing levels of $[Ca^{2+}]_{ER}$, we expressed an EF-hStim1 mutant, D76A-hStim1, which is insensitive to $[Ca^{2+}]_{ER}$ levels (Liou *et al.*, 2005). Coexpression of D76A-hStim1+hOrai1 increased basal $[Ca^{2+}]_i$ in GV oocytes, but, unlike the case for previous treatments, basal $[Ca^{2+}]_i$ did not decrease, but effectively increased, as oocytes progressed to the MII stage ($p < 0.05$; Figure 6B, bottom, right).

Regulation of Ca^{2+} influx is required to complete oocyte maturation

We then examined whether the distinct basal $[Ca^{2+}]_i$ profiles generated by expression of one or both of the SOCE components had differential effects on the rates of in vitro maturation. To accomplish this, we momentarily maintained control GV oocytes or oocytes injected with the selected cRNAs at the GV stage to allow for protein translation, after which in vitro maturation proceeded for 14–16 h. The majority of control oocytes, ~80%, resumed meiosis and reached the MII stage (Figure 7A), although oocytes expressing hStim1 or hStim1+hOrai1, which displayed elevated basal $[Ca^{2+}]_i$ at the GV stage, showed reduced rates of maturation, with more oocytes remaining arrested at the GV stage ($p < 0.05$). Remarkably, oocytes expressing D76A hStim1+hOrai1, which displayed persistent elevation of basal $[Ca^{2+}]_i$, failed to consistently resume meiosis (Figure 7A).

To examine whether the excessive Ca^{2+} influx caused by coexpression of D76A hStim1+ hOrai1 was responsible for the GV arrest, we repeated the foregoing experiment but 2.5 h after release from IBMX oocytes were transferred to medium containing 0.4 mM $CaCl_2$. Under normal $[Ca^{2+}]_e$, as expected, all control oocytes reached the GVBD stage by 2.5 h, although only ~25% of oocytes expressing D76AhStim1+hOrai1 did (Figure 7B; $p < 0.05$). Subsequently, all D76A-hStim1+hOrai1–expressing oocytes maintained in normal $[Ca^{2+}]_e$-containing media remained arrested at the GV stage, whereas cohort oocytes transferred to 0.4 mM $CaCl_2$-containing media progressively underwent GVBD, and by 12 h, ~50% had undergone GVBD (Figure 7C); progression of maturation in control oocytes was not affected by 0.4 mM $CaCl_2$ media (Figure 7C). We then examined whether moving oocytes to 0.4 mM $CaCl_2$ media altered basal $[Ca^{2+}]_i$. As shown in Figure 7, D and E, 2 h after changing media oocytes expressing D76A hStim1+hOrai1 displayed a significantly lower basal $[Ca^{2+}]_i$ ($p < 0.05$), whereas control oocytes were not affected by the switch. Taken together, these results suggest that regulation of Ca^{2+} influx and Ca^{2+} homeostasis play a role during normal progression of meiosis in mouse oocytes.

DISCUSSION

In this study we examined how $[Ca^{2+}]_e$ and Ca^{2+} influx contribute to $[Ca^{2+}]_{ER}$ content during mouse oocyte maturation. We also investigated the presence and function of SOCE and the effect of Ca^{2+} influx misregulation on oocyte maturation. We found that whereas $[Ca^{2+}]_{ER}$ levels increase during maturation, Ca^{2+} entry declines. We detected expression of Stim1 and Orai1 in oocytes and eggs, as well as a change in their distribution such that hStim1-YFP and hOrai1-mRFP only extensively overlapped in GV oocytes after addition of TG. Finally, expression of hStim1+hOrai1 increased basal $[Ca^{2+}]_i$ in GV oocytes but not in MII eggs and persistently elevated basal $[Ca^{2+}]_i$ compromised oocyte maturation. In total, our studies demonstrate that Ca^{2+} influx is closely regulated during oocyte maturation and that alteration of Ca^{2+} homeostasis undermines the completion of maturation.

$[Ca^{2+}]_{ER}$, $[Ca^{2+}]_i$ influx, and SOCE during mouse oocyte maturation

Although $[Ca^{2+}]_{ER}$ levels have been known to increase during mouse oocyte maturation, the source of Ca^{2+} and the Ca^{2+} influx mechanism(s) underlying this increase have not been established. Here we show that $[Ca^{2+}]_e$ is required for the increase in $[Ca^{2+}]_{ER}$ and that as $[Ca^{2+}]_{ER}$ increases during maturation, spontaneous or TG-induced Ca^{2+} influx decreases; Ca^{2+} influx is lowest at the MII stage, which is when $[Ca^{2+}]_{ER}$ is greatest. This relationship between $[Ca^{2+}]_{ER}$ and Ca^{2+} influx, which is especially evident at the GV and GVBD stages, suggests participation of SOCE and is reminiscent of data for *Xenopus*, in which SOCE-mediated Ca^{2+} entry is abruptly inactivated at the GVBD stage (Machaca and Haun, 2000, 2002). Our results, unlike those for *Xenopus*, show that SOCE is only partly inactivated by the GVBD stage and can contribute to the increase in $[Ca^{2+}]_{ER}$ during this period. Our results differ from other studies in the mouse showing progressively enhanced SOCE activity during maturation (Gomez-Fernandez *et al.*, 2009, 2012).

Several additional findings in our study suggest a role for SOCE during mouse oocyte maturation. For example, addition of 2-APB, a broad-spectrum SOCE inhibitor (DeHaven *et al.*, 2008; Putney, 2010), abrogated Ca^{2+} influx in GV oocytes. Moreover, both Stim1 and Orai1 were produced by oocytes throughout maturation, and expression of functional hStim1 caused enhanced Ca^{2+} influx, whereas an inactive form, hStim1-ΔCAD-YFP, failed to promote Ca^{2+} influx. In spite of such findings indicating a role of SOCE during oocyte maturation, the progressive inactivation of SOCE during maturation raises questions regarding its contribution to Ca^{2+} influx during fertilization. Recent research in mouse eggs suggests a minor role for SOCE during fertilization, for, although it was functional in MII eggs, abrogating its function by pharmacological and molecular means failed to modify sperm-initiated oscillations (Miao *et al.*, 2012; Takahashi *et al.*, 2013). Of importance, in porcine oocytes, inactivation of SOCE by small interfering RNA against Stim1 and Orai1 inhibited persistent fertilization-associated oscillations (Lee *et al.*, 2012; Wang *et al.*, 2012). Taken together, these results suggest that in mammals different Ca^{2+} influx mechanisms regulate $[Ca^{2+}]_{ER}$ during maturation and Ca^{2+} influx during fertilization, and future studies should identify these channels and their regulation.

Reorganization of hStim1 and hOrai1 during oocyte maturation

The inactivation of spontaneous and SOCE-mediated Ca^{2+} influx led us to examine whether changes in the distribution of Stim1 and Orai1 could be undermining Ca^{2+} influx. Given the inconsistent results obtained using immunofluorescence to localize endogenous Stim1 (data not shown), we used corresponding mRNAs also encoding fluorescent proteins. Marked changes in the organization of these proteins began around GVBD. For example, in GV oocytes internal "patches" and peri-GV accumulation highlighted the widespread distribution of hStim1, but after GVBD and for the rest of maturation, hStim1 distribution became diffuse and acquired a reticular, ER-like pattern consistent with its localization. Further, addition of TG, which in GV oocytes caused hStim1 to diffuse to the cortex and form distinct puncta, hardly changed the distribution of hStim1 in eggs. The distribution of Orai1 also changed, as in GV

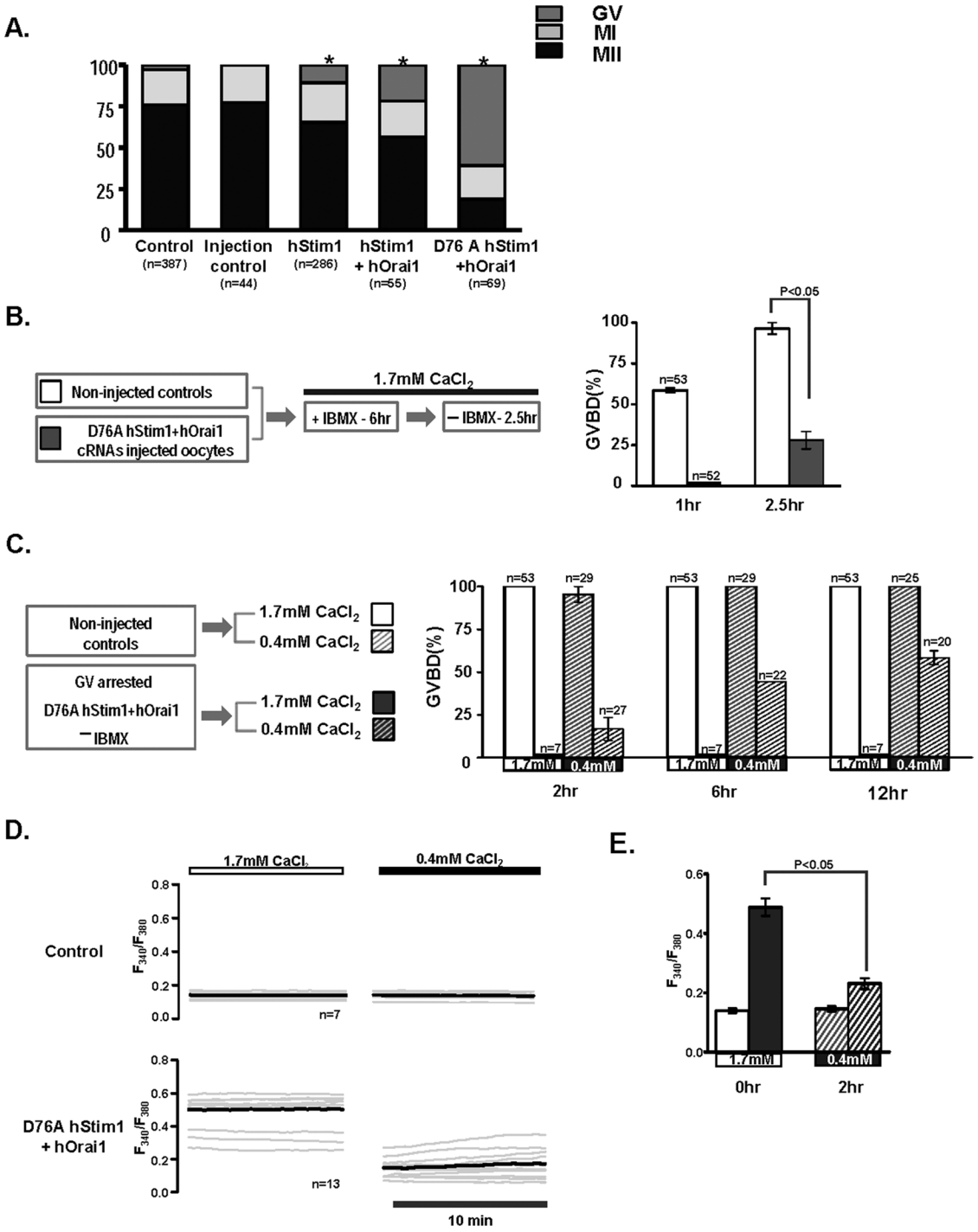

FIGURE 7: Changes in Ca^{2+} homeostasis affect resumption of meiosis and oocyte maturation. (A) Control, sham-injected, and oocytes expressing hStim1-YFP, hStim1-YFP+hOrai1-mRFP, or D76A Stim1-YFP+hOrai1-mRFP were in vitro matured and their maturation rates assessed. Expression of any mRNAs that increased basal $[Ca^{2+}]_i$ even transiently caused a reduction in maturation rates, although expression D76A hStim1-YFP+hOrai1-mRFP nearly completely prevented resumption of meiosis. Asterisks above bars represent treatments that significantly reduced GVBD rates ($p < 0.05$). (B) The effect of coexpression of D76A hStim1-YFP + hOrai1-mRFP on meiotic resumption was investigated as depicted in the flow chart (left), and data are summarized in the bar graph (right). Expression of D76A hStim1-YFP+hOrai1-mRFP in GV oocytes delayed and mostly prevented GVBD under normal $[Ca^{2+}]_e$ ($p < 0.05$). (C) As before, but selected GV-arrested oocytes were transferred to low-$[Ca^{2+}]_e$ medium (0.4 mM), which partly rescued the arrest caused by expression of D76A hStim1-YFP+hOrai1-mRFP. (D) Ca^{2+} traces depicting the effect of lowering $[Ca^{2+}]_e$ on basal $[Ca^{2+}]_i$ in control and GV-arrested D76A hStim1+hOrai1–expressing oocytes monitored before and 2 h after lowering $[Ca^{2+}]_e$ from 1.7 to 0.4 mM; the bold trace represents the mean of the responses. (E) A bar graph was used to summarize in the same group of oocytes the mean ± SEM change in basal $[Ca^{2+}]_i$ caused by lowering external $[Ca^{2+}]_e$; $p < 0.05$.

oocytes it was primarily present on the PM, but by MII its PM presence was reduced and its signal in the ooplasm increased. In agreement with these changes, after addition of TG, hStim1 and hOrai1 only colocalized on the PM of GV oocytes. Our results are in agreement with those in *Xenopus* oocytes, where inactivation of SOCE during maturation was associated with inhibition of Stim1 oligomerization/puncta formation and Orai1 internalization (Yu *et al.*, 2009, 2010). Nevertheless, our results show that hStim1 retained certain clustering capacity and Orai1 internalization was incomplete in MII eggs, as even at this stage expression of hStim1+hOrai1 enhanced SOCE activity. Our results also concur with data in somatic cells, where SOCE is down-regulated at mitosis (Russa *et al.*, 2008; Smyth *et al.*, 2009) and this change was associated with reduced ability of Stim1 to form puncta (Smyth *et al.*, 2009). Data from studies in mammalian oocytes also support our findings. For example, after depletion of $[Ca^{2+}]_{ER}$ Stim1 displayed some degree of oligomerization in porcine MII eggs (Koh *et al.*, 2009), and in mouse eggs Stim1 showed conspicuous clusters/puncta organization, although without emptying of the stores, and Orai1 distribution was mostly concentrated at the PM (Gomez-Fernandez *et al.*, 2012).

We did not investigate the mechanisms that regulate Stim1 reorganization in oocytes. Nevertheless, Stim1 was originally described as a phosphoprotein (Manji *et al.*, 2000), and phosphorylation of its S/T-P consensus sites by M-phase kinases was demonstrated in somatic cells (Manji *et al.*, 2000; Smyth *et al.*, 2009; Pozo-Guisado *et al.*, 2010) and *Xenopus* oocytes (Yu *et al.*, 2009). We found that exogenous hStim1 was phosphorylated in MII eggs, as it experienced a mobility shift that was reduced by phosphatase treatment. We did not observe similar changes in the endogenous protein, although the comparable temporal inactivation of TG-induced Ca^{2+} influx between uninjected and hStim1 mRNA–injected oocytes suggest common regulatory mechanisms.

Ca^{2+} influx and progression of oocyte maturation

To gain further insight into the mechanisms underlying the brief presence of $[Ca^{2+}]_i$ oscillations in GV stage mouse oocytes (Carroll and Swann, 1992; Carroll *et al.*, 1994), we expressed, singly or together, hStim1 and hOrai1 mRNAs and monitored their effects on basal $[Ca^{2+}]_i$ in oocytes and eggs. We found that their combined expression markedly and persistently increased basal $[Ca^{2+}]_i$ in GV oocytes, although by the MII stage, basal $[Ca^{2+}]_i$ levels had returned to near-normal levels. These results suggest close regulation of Ca^{2+} homeostasis/influx during the early stages of maturation.

To better understand the role of basal $[Ca^{2+}]_i$ and Ca^{2+} influx on oocyte maturation, we coexpressed D76A hStim1+hOrai1 mRNAs, which increased basal $[Ca^{2+}]_i$ throughout maturation. Under these conditions, progression of maturation was greatly reduced, with most oocytes remaining at the GV stage. These effects were due to the inability to inactivate Ca^{2+} influx and decrease basal $[Ca^{2+}]_i$, as lowering external $[Ca^{2+}]_e$ reduced $[Ca^{2+}]_i$ and rescued the ability of these oocytes to undergo GVBD. Similar detrimental effects of elevated basal $[Ca^{2+}]_i$ were observed in *Xenopus* oocytes, where enhanced Ca^{2+} influx promoted throughout maturation hindered the progression of meiosis (Sun and Machaca, 2004). Therefore it appears that regulation of Ca^{2+} influx is required for normal progression of oocyte maturation in the mouse, although we did not explore the functional mechanism(s) positively affected by the progressive inactivation of Ca^{2+} entry.

We propose a model in which mouse GV oocytes exhibit a low but persistent Ca^{2+} influx that contributes to the GV's overall cellular metabolism. On resumption of meiosis, Ca^{2+} influx is progressively inactivated to allow for normal progression of meiosis, spindle organization, and MII arrest. Future studies in mammalian oocytes should elucidate the mechanism(s) responsible for the inactivation of Ca^{2+} influx and the identity of the channel(s) that mediate Ca^{2+} entry during maturation and fertilization.

MATERIALS AND METHODS

Collection and preparation of mouse oocytes

Fully grown GV-stage oocytes were collected from the ovaries of 6- to 10-wk-old CD-1 female mice 44–46 h after injection of 5 IU of pregnant mare serum gonadotropin (PMSG; Sigma-Aldrich, St. Louis, MO; all chemicals are from Sigma-Aldrich unless otherwise indicated), as we previously described (Kurokawa *et al.*, 2007). Cumulus intact GVs were recovered into a 4-(2-hydroxyethyl)-1-piperazineethanesulfonic acid (HEPES)–buffered Tyrode's lactate solution (TL-HEPES) containing 5% fetal calf serum (Invitrogen, Carlsbad, CA) and supplemented with 100 µM IBMX to block spontaneous progression of meiosis. When necessary, cumulus cells were removed by repetitive pipetting using a fine capillary glass. Oocytes were matured in vitro for 12–14 h in IBMX-free Chatot, Ziomek, and Bavister medium (CZB; Chatot *et al.*, 1989) supplemented with 3 mg/ml bovine serum albumin (BSA) or 0.02% polyvinyl alcohol (average molecular weight 30,000–70,000) under paraffin oil at 36.5°C in a humidified atmosphere containing 6% CO_2. In vivo–matured MII oocytes were collected from the oviducts 12–14 h after administration of 5 IU of human chorionic gonadotropin, which was injected 46–48 h after PMSG. All procedures were performed according to research animal protocols approved by the University of Massachusetts Institutional Animal Care and Use Committee.

Generation of constructs and mRNA preparation

hStim1-YFP and hOrai1 were generously provided by T. Meyer (Stanford University, Stanford, CA) and M. Trebak (Albany Medical College, Albany, NY), respectively. hStim1-YFP was subcloned into a pcDNA6/Myc-His B vector (Invitrogen) between the restrictions sites *Age*I and *Xba*I. The hOrai1 insert was amplified by PCR and ligated to the N-terminus of the mRFP-bearing pcDNA6/Myc-His B vector (D. Alfandari, University of Massachusetts, Amherst, MA) between *Eco*RI and *Xho*I restriction sites. Constitutively active hStim1, D76A hStim1-YFP, and hStim1-482 stop were generated either by substituting D76 to A or introducing the stop codon after amino acid 481 using the QuikChange Site-Directed Mutagenesis Kit (Stratagene, La Jolla, CA), as previously reported (Liou *et al.*, 2005; Smyth *et al.*, 2009). Before performing in vitro transcription reactions, we verified the sequences of all new constructs and presence of targeted mutations by DNA sequencing. Constructs were linearized outside of the coding region with *Pme*I and in vitro transcribed using T7 mMESSAGE mMACHINE Kit (Ambion, Austin, TX). A poly(A) tail was added to the mRNAs using a Tailing Kit (Ambion). All mRNAs were prepared to final concentrations of 1.5 µg/µl, aliquoted, and frozen at −80°C until use.

Microinjection of mRNAs

Microinjections were performed as described previously by our laboratory (Kurokawa *et al.*, 2007). Before injection, cRNAs were heat denatured and centrifuged, and the top 1.2 µl was used to prepare microdrops from which glass micropipettes were loaded by aspiration. cRNAs were delivered into oocytes using pneumatic pressure (PLI-100 picoinjector; Harvard Apparatus, Holliston, MA). When cRNAs were injected simultaneously, as in the case of hOrai1–mRFP+hStim1-YFP or hOrai1-mRFP+D76A hStim1-YFP, cRNAs were mixed immediately before the injection procedure in 1–3 M ratios, respectively, to allow similar protein expression, which

was estimated by comparing fluorescence intensities. When injections were performed in GV oocytes and to allow for maximal translation, oocytes were kept in CZB plus IBMX for 6 h, after which IBMX was removed to allow the commencement of maturation. GVBD- and MI-stage oocytes were maturated for 4 and 8 h, respectively, whereas MII oocytes were matured for 12–14 h in CZB.

$[Ca^{2+}]_i$ measurements and Ca^{2+} reagents

$[Ca^{2+}]_i$ monitoring was performed as previously reported by our laboratory (Kurokawa *et al.*, 2007). In brief, Fura-2 acetoxymethyl ester (Fura-2AM) was loaded by incubating oocytes in a HEPES-buffered CZB solution (HCZB) containing 1.25 μM Fura-2AM for 20 min at room temperature. Oocytes were then immobilized on glass-bottom dishes (MatTek Corp., Ashland, MA) and placed on the stage of an inverted microscope (Nikon, Melville, NY). Fura-2 fluorescence was excited with 340- and 380-nm wavelengths every 20 s, and emitted light was collected at wavelengths >510 nm by a cooled Photometrics SenSys charge-coupled device camera (Roper Scientific, Tucson, AZ). Acquisition of fluorescence ratios and rotation of the filter wheel were controlled by Simple PCI software (C-Imaging System Software, Cranberry Township, PA).

To examine the role of Ca^{2+} influx on refilling of $[Ca^{2+}]_{ER}$, we placed IBMX-treated GV oocytes in CZB medium either with or without 1.7 mM $CaCl_2$ and allowed them to mature for 4 h, after which we placed them in nominal Ca^{2+}-free HCZB and after a 5-min interval assessed interval $[Ca^{2+}]_{ER}$ levels by adding TG (Calbiochem, San Diego, CA), an inhibitor of the SERCA pump, which induced Ca^{2+} leak by an unknown mechanism. TG-induced Ca^{2+} rises were regarded as $[Ca^{2+}]_{ER}$ content that could be estimated from the area under the curve of the $[Ca^{2+}]_i$ rise using Prism software (GraphPad Software, La Jolla, CA). To estimate SOCE and assess the effect of $[Ca^{2+}]_{ER}$ on hStim1-YFP distribution, we followed oocytes by the method in Bird *et al.* (2008). Before adding 10 μM TG, we placed oocytes in Ca^{2+}-free HCZB supplemented with 1 mM ethylene glycol tetraacetic acid (EGTA). When $[Ca^{2+}]_i$ returned to near baseline values, ~35 min after TG addition, 5 mM $CaCl_2$ was added to the medium, and the amplitude of the $[Ca^{2+}]_i$ rise caused by the addition was used to estimate SOCE.

Western blotting procedures

To detect endogenous/exogenous Stim1 and Orai1, we prepared protein lysates from 200 or 20–45, respectively, GV or MII oocytes. Oocytes were washed in Dulbecco's phosphate-buffered saline (DPBS), lysed in 2× sample buffer, and stored at −20°C until use. Heat-denatured proteins (95°C for 3 min) were separated by 7.5 or 10% SDS–PAGE and transferred to polyvinylidene fluoride membranes (Millipore, Bedford, MA). Membranes were blocked with 6% skim milk dissolved in PBS plus 0.1% Tween-20 for 2 h at 4°C. Two different antibodies were used against Stim1, one raised to recognize the N-terminus (1:100; BD Biosciences, San Jose, CA) and the other to identify the C-terminus end of the molecule (1:500; ProSci, Poway, CA), for which a blocking antigenic peptide (AP) was available. Orai1 was detected using an anti-Orai1 antibody (1:300; ProSci) raised against the C-terminus of the molecule, and an AP was also available for this antibody. For these experiments, equal volumes of AP (ProSci) and of the specific antibody were incubated for 2 h at 4°C, after which this mixture was used to complete the Western blotting procedure. In all samples, an anti-actin antibody was used to detect actin reactivity, which was used as a loading control (1:500; Millipore). Blots were incubated overnight at 4°C with primary antibodies, and goat anti-mouse or anti-rabbit antibodies conjugated with horseradish peroxidase were used as secondary antibodies (1:2000; Bio-Rad, Hercules, CA) and incubated for 1 h at room temperature. The membranes were then exposed to chemiluminescence reagents (NEN Life Science Products, Boston, MA) and the signal assessed using a Kodak 440 Image Station (Rochester, NY). The same anti-Stim1 antibodies were used to detect exogenously expressed hStim1-YFP (n = 45), which were also detected using an anti-GFP antibody (1:1000; MBL, Woburn, MA).

Phosphatase treatment was carried out on wild-type hStim1-YFP–expressing GV and MII oocytes/eggs. Samples were washed in DPBS and placed in phosphatase buffer (50 mM Tris-HCl, 100 mM NaCl, 10 mM $MgCl_2$,and 1 mM dithiothreitol) supplemented with a protease inhibitor cocktail (Roche, Indianapolis, IN); control samples were also supplemented with 50 mM β-glycerophosphate to inhibit endogenous phosphatases. All samples were lysed by repeated cycles of freezing and thawing using liquid nitrogen, and 0.5 U of calf intestine phosphatase (New England BioLabs, Ipswich, MA) was added to the indicated groups; all samples were incubated at 37°C for 30 min. The reaction was stopped by addition of 2× sample buffer, after which Western blotting was performed as described.

Plasma membrane staining

To estimate the proximity of hStim1-YFP puncta to the PM during the different stages of maturation, we stained the PM of oocytes/eggs using 10 μg/ml wheat germ agglutinin conjugated with Alexa Fluor 633 (Invitrogen) according to manufacturer's instructions. Before staining, the zona pellucida was removed using Tyrode's acidic solution, pH 2.5, to facilitate the diffusion of the stain. ImageJ (National Institutes of Health, Bethesda, MD) software was used to quantify the distances of the hStim1 puncta to the PM in micrometers and the diameters of hStim1 aggregates and to draw the line scan to compare hOrai1 PM distribution.

Live imaging of oocytes using confocal microscope

Oocytes/eggs expressing proteins tagged with fluorescent proteins were collected at variable times of maturation and attached to glass-bottom dishes while incubated in BSA-free HCZB medium. Fluorescence was examined using an LSM 510 META confocal microscope (Carl Zeiss Microimaging, Jena, Germany) outfitted with a 63×/1.4 numerical aperture oil immersion lens. Images were taken at the equatorial and cortical regions of oocytes/eggs.

Statistical analysis

Statistical analysis was performed using Prism software (GraphPad, La, Jolla, CA). All data are presented as mean ± SEM. Mean data were compared using unpaired t test or analysis of variance, as appropriate. Categorical values such as those generated by maturation rates were analyzed using the chi-square test. p <0.05 was considered significant.

ACKNOWLEDGMENTS

These studies were supported in part by Grant HD051872 from the National Institutes of Health to R.A.F. We thank Nan Zhang for useful discussions and Changli He for overall technical support.

REFERENCES

Balghi H *et al.* (2011). Enhanced Ca^{2+} entry due to Orai1 plasma membrane insertion increases IL-8 secretion by cystic fibrosis airways. FASEB J 25, 4274–4291.

Berridge MJ, Lipp P, Bootman MD (2000). The versatility and universality of calcium signalling. Nat Rev Mol Cell Biol 1, 11–21.

Bird GS, DeHaven WI, Smyth JT, Putney JW Jr (2008). Methods for studying store-operated calcium entry. Methods 46, 204–212.

Carroll J, Swann K (1992). Spontaneous cytosolic calcium oscillations driven by inositol trisphosphate occur during in vitro maturation of mouse oocytes. J Biol Chem 267, 11196–11201.
Carroll J, Swann K, Whittingham D, Whitaker M (1994). Spatiotemporal dynamics of intracellular $[Ca^{2+}]_i$ oscillations during the growth and meiotic maturation of mouse oocytes. Development 120, 3507–3517.
Chatot CL, Ziomek CA, Bavister BD, Lewis JL, Torres I (1989). An improved culture medium supports development of random-bred 1-cell mouse embryos in vitro. J Reprod Fertil 86, 679–688.
Collins SR, Meyer T (2011). Evolutionary origins of STIM1 and STIM2 within ancient Ca^{2+} signaling systems. Trends Cell Biol 21, 202–211.
Darbellay B, Arnaudeau S, Bader CR, Konig S, Bernheim L (2011). STIM1L is a new actin-binding splice variant involved in fast repetitive Ca^{2+} release. J Cell Biol 194, 335–346.
DeHaven WI, Smyth JT, Boyles RR, Bird GS, Putney JW Jr (2008). Complex actions of 2-aminoethyldiphenyl borate on store-operated calcium entry. J Biol Chem 283, 19265–19273.
Ducibella T, Fissore R (2008). The roles of Ca^{2+}, downstream protein kinases, and oscillatory signaling in regulating fertilization and the activation of development. Dev Biol 315, 257–279.
Feske S, Gwack Y, Prakriya M, Srikanth S, Puppel SH, Tanasa B, Hogan PG, Lewis RS, Daly M, Rao A (2006). A mutation in Orai1 causes immune deficiency by abrogating CRAC channel function. Nature 441, 179–185.
Gomez-Fernandez C, Lopez-Guerrero AM, Pozo-Guisado E, Alvarez IS, Martin-Romero FJ (2012). Calcium signaling in mouse oocyte maturation: the roles of STIM1, ORAI1 and SOCE. Mol Hum Reprod 18, 194–203.
Gomez-Fernandez C, Pozo-Guisado E, Ganan-Parra M, Perianes MJ, Alvarez IS, Martin-Romero FJ (2009). Relocalization of STIM1 in mouse oocytes at fertilization: early involvement of store-operated calcium entry. Reproduction 138, 211–221.
Gwack Y, Srikanth S, Feske S, Cruz-Guilloty F, Oh-hora M, Neems DS, Hogan PG, Rao A (2007). Biochemical and functional characterization of Orai proteins. J Biol Chem 282, 16232–16243.
Homa ST (1991). Neomycin, an inhibitor of phosphoinositide hydrolysis, inhibits the resumption of bovine oocyte spontaneous meiotic maturation. J Exp Zoology 258, 95–103.
Hoth M, Penner R (1993). Calcium release-activated calcium current in rat mast cells. J Physiol 465, 359–386.
Hsu S, O'Connell PJ, Klyachko VA, Badminton MN, Thomson AW, Jackson MB, Clapham DE, Ahern GP (2001). Fundamental Ca^{2+} signaling mechanisms in mouse dendritic cells: CRAC is the major Ca^{2+} entry pathway. J Immunol 166, 6126–6133.
Jones KT, Carroll J, Whittingham DG (1995). Ionomycin, thapsigargin, ryanodine, and sperm induced Ca^{2+} release increase during meiotic maturation of mouse oocytes. J Biol Chem 270, 6671–6677.
Kaufman ML, Homa ST (1993). Defining a role for calcium in the resumption and progression of meiosis in the pig oocyte. J Exp Zool 265, 69–76.
Kline D, Kline JT (1992). Thapsigargin activates a calcium influx pathway in the unfertilized mouse egg and suppresses repetitive calcium transients in the fertilized egg. J Biol Chem 267, 17624–17630.
Koh S, Lee K, Wang C, Cabot RA, Machaty Z (2009). STIM1 regulates store-operated Ca^{2+} entry in oocytes. Dev Biol 330, 368–376.
Kurokawa M, Yoon SY, Alfandari D, Fukami K, Sato K, Fissore RA (2007). Proteolytic processing of phospholipase Czeta and $[Ca^{2+}]_i$ oscillations during mammalian fertilization. Dev Biol 312, 407–418.
Lee K, Wang C, Machaty Z (2012). STIM1 is required for Ca^{2+} signaling during mammalian fertilization. Dev Biol 367, 154–162.
Liou J, Kim ML, Heo WD, Jones JT, Myers JW, Ferrell JE Jr, Meyer T (2005). STIM is a Ca^{2+} sensor essential for Ca^{2+}-store-depletion-triggered Ca^{2+} influx. Curr Biol 15, 1235–1241.
Machaca K, Haun S (2000). Store-operated calcium entry inactivates at the germinal vesicle breakdown stage of *Xenopus* meiosis. J Biol Chem 275, 38710–38715.
Machaca K, Haun S (2002). Induction of maturation-promoting factor during *Xenopus* oocyte maturation uncouples Ca^{2+} store depletion from store-operated Ca^{2+} entry. J Cell Biol 156, 75–85.
Malcuit C, Kurokawa M, Fissore RA (2006). Calcium oscillations and mammalian egg activation. J Cell Physiol 206, 565–573.
Manji SS, Parker NJ, Williams RT, van Stekelenburg L, Pearson RB, Dziadek M, Smith PJ (2000). STIM1: a novel phosphoprotein located at the cell surface. Biochim Biophys Acta 1481, 147–155.
McGuinness OM, Moreton RB, Johnson MH, Berridge MJ (1996). A direct measurement of increased divalent cation influx in fertilised mouse oocytes. Development 122, 2199–2206.
Mehlmann LM, Kline D (1994). Regulation of intracellular calcium in the mouse egg: calcium release in response to sperm or inositol trisphosphate is enhanced after meiotic maturation. Biol Reprod 51, 1088–1098.
Miao YL, Stein P, Jefferson WN, Padilla-Banks E, Williams CJ (2012). Calcium influx-mediated signaling is required for complete mouse egg activation. Proc Natl Acad Sci USA 109, 4169–4174.
Miyazaki S (2006). Thirty years of calcium signals at fertilization. Semin Cell Dev Biol 17, 233–243.
Miyazaki S, Shirakawa H, Nakada K, Honda Y (1993). Essential role of the inositol 1,4,5-trisphosphate receptor/Ca^{2+} release channel in Ca^{2+} waves and Ca^{2+} oscillations at fertilization of mammalian eggs. Dev Biol 158, 62–78.
Miyazaki S, Yuzaki M, Nakada K, Shirakawa H, Nakanishi S, Nakade S, Mikoshiba K (1992). Block of Ca^{2+} wave and Ca^{2+} oscillation by antibody to the inositol 1,4,5-trisphosphate receptor in fertilized hamster eggs. Science 257, 251–255.
Mohri T, Shirakawa H, Oda S, Sato MS, Mikoshiba K, Miyazaki S (2001). Analysis of Mn^{2+}/Ca^{2+} influx and release during Ca^{2+} oscillations in mouse eggs injected with sperm extract. Cell Calcium 29, 311–325.
Parekh AB, Fleig A, Penner R (1997). The store-operated calcium current I_{CRAC}: nonlinear activation by $InsP_3$ and dissociation from calcium release. Cell 89, 973–980.
Park CY, Hoover PJ, Mullins FM, Bachhawat P, Covington ED, Raunser S, Walz T, Garcia KC, Dolmetsch RE, Lewis RS (2009). STIM1 clusters and activates CRAC channels via direct binding of a cytosolic domain to Orai1. Cell 136, 876–890.
Penna A, Demuro A, Yeromin AV, Zhang SL, Safrina O, Parker I, Cahalan MD (2008). The CRAC channel consists of a tetramer formed by Stim-induced dimerization of Orai dimers. Nature 456, 116–120.
Pozo-Guisado E, Campbell DG, Deak M, Alvarez-Barrientos A, Morrice NA, Alvarez IS, Alessi DR, Martin-Romero FJ (2010). Phosphorylation of STIM1 at ERK1/2 target sites modulates store-operated calcium entry. J Cell Sci 123, 3084–3093.
Prakriya M, Feske S, Gwack Y, Srikanth S, Rao A, Hogan PG (2006). Orai1 is an essential pore subunit of the CRAC channel. Nature 443, 230–233.
Putney JW ((2009). Capacitative calcium entry: from concept to molecules. Immunol Rev 231, 10–22.
Putney JW ((2010). Pharmacology of store-operated calcium channels. Mol Interv 10, 209–218.
Putney JW Jr (1986). A model for receptor-regulated calcium entry. Cell Calcium 7, 1–12.
Roos J *et al.* (2005). STIM1, an essential and conserved component of store-operated Ca^{2+} channel function. J Cell Biol 169, 435–445.
Runft LL, Jaffe LA, Mehlmann LM (2002). Egg activation at fertilization: where it all begins. Dev Biol 245, 237–254.
Russa AD, Ishikita N, Masu K, Akutsu H, Saino T, Satoh Y (2008). Microtubule remodeling mediates the inhibition of store-operated calcium entry (SOCE) during mitosis in COS-7 cells. Arch Histol Cytol 71, 249–263.
Saunders CM, Larman MG, Parrington J, Cox LJ, Royse J, Blayney LM, Swann K, Lai FA (2002). PLC zeta: a sperm-specific trigger of Ca^{2+} oscillations in eggs and embryo development. Development 129, 3533–3544.
Smyth JT, Petranka JG, Boyles RR, DeHaven WI, Fukushima M, Johnson KL, Williams JG, Putney JW Jr (2009). Phosphorylation of STIM1 underlies suppression of store-operated calcium entry during mitosis. Nat Cell Biol 11, 1465–1472.
Stricker SA (1999). Comparative biology of calcium signaling during fertilization and egg activation in animals. Dev Biol 211, 157–176.
Sun L, Machaca K (2004). $Ca^{2+}{}_{cyt}$ negatively regulates the initiation of oocyte maturation. J Cell Biol 165, 63–75.
Swann K, Saunders CM, Rogers NT, Lai FA (2006). PLCζ(zeta): a sperm protein that triggers Ca^{2+} oscillations and egg activation in mammals. Semin Cell Dev Biol 17, 264–273.
Takahashi T, Kikuchi T, Kidokoro Y, Shirakawa H (2013). Ca^{2+} influx-dependent refilling of intracellular Ca^{2+} stores determines the frequency of Ca^{2+} oscillations in fertilized mouse eggs. Biochem Biophys Res Commun 430, 60–65.
Takemura H, Hughes AR, Thastrup O, Putney JW Jr (1989). Activation of calcium entry by the tumor promoter thapsigargin in parotid acinar cells. Evidence that an intracellular calcium pool and not an inositol phosphate regulates calcium fluxes at the plasma membrane. J Biol Chem 264, 12266–12271.

Tombes RM, Simerly C, Borisy GG, Schatten G (1992). Meiosis, egg activation, and nuclear envelope breakdown are differentially reliant on Ca^{2+}, whereas germinal vesicle breakdown is Ca^{2+} independent in the mouse oocyte. J Cell Biol 117, 799–811.

Vig M *et al*. (2006). CRACM1 multimers form the ion-selective pore of the CRAC channel. Curr Biol 16, 2073–2079.

Wang C, Lee K, Gajdocsi E, Papp AB, Machaty Z (2012). Orai1 mediates store-operated Ca^{2+} entry during fertilization in mammalian oocytes. Dev Biol 365, 414–423.

Yu F, Sun L, Machaca K (2009). Orai1 internalization and STIM1 clustering inhibition modulate SOCE inactivation during meiosis. Proc Natl Acad Sci USA 106, 17401–17406.

Yu F, Sun L, Machaca K (2010). Constitutive recycling of the store-operated Ca^{2+} channel Orai1 and its internalization during meiosis. J Cell Biol 191, 523–535.

Zweifach A, Lewis RS (1993). Mitogen-regulated Ca^{2+} current of T lymphocytes is activated by depletion of intracellular Ca^{2+} stores. Proc Natl Acad Sci USA 90, 6295–6299.